


# A Bayesian Approach for Extracting Fluorescence Lifetimes from Sparse Data Sets and Its Significance for Imaging Experiments

Kalyan Santra<sup>1,2</sup> , Emily A. Smith<sup>1,2</sup>, Xueyu Song<sup>1,2</sup> and Jacob W. Petrich<sup>\*1,2</sup>

<sup>1</sup>Department of Chemistry, Iowa State University, Ames, IA

<sup>2</sup>Ames Laboratory, U.S. Department of Energy, Ames, IA

Received 26 June 2018, accepted 6 November 2018, DOI: 10.1111/php.13057

## ABSTRACT

The measurement of fluorescence lifetimes, especially in small sample volumes, presents the dual challenge of probing a small number of fluorophores and fitting the concomitant sparse data set to the appropriate excited-state decay function. A common method of analysis, such as the maximum likelihood (ML) technique, assumes a *uniform* probability distribution of the parameters describing the fluorescence decay function. An improvement is thus suggested by implementing a suitable *nonuniform* distribution, as is provided by a Bayesian framework, where the distribution of parameters is obtained from both their prior knowledge and the evidence-based likelihood of an event for a given set of parameters. We have also considered the Dirichlet prior distribution, whose mathematical form enables analytical solutions of the fitting parameters to be rapidly obtained. If Gaussian and exponential prior distributions are judiciously chosen, they reproduce the experimental target lifetime to within 20% with as few as 20 total photon counts for the data set, as does the Dirichlet prior distribution. But because of the analytical solutions afforded by the Dirichlet prior distribution, it is proposed to employ a Dirichlet prior to search parameter space rapidly to provide, if necessary, appropriate parameters for subsequent employment of a Gaussian or exponential prior distribution.

## INTRODUCTION

Time-correlated, single-photon counting has become an integral part of techniques such as fluorescence-lifetime imaging microscopy (1–5), Förster resonance energy transfer (6–8) and fluorescence correlation spectroscopy (9–11). The technique records the time difference between the arrival times of an excitation pulse and a pulse resulting from a photon detected from fluorescence emission. A histogram of arrival-time differences is accumulated and fit to a model function for the fluorescence decay. The most frequently used fitting method (residual minimization, RM) minimizes the weighted squares of the residuals of the experimental data and the continuously optimized fitting function. RM requires a histogram of very high quality to extract the mean lifetime with high accuracy, and such a histogram is only obtained with a large number of total photon counts (~20 000 for rose bengal).

In super-resolution microscopies, however, such as stimulated emission depletion microscopy (12–14), high spatial resolution is only obtained at the expense of the fluorescence signal, as the latter decreases with decreasing detection volume. Additional factors such as a low intrinsic fluorescence quantum yield or photodegradation of the sample contribute to reducing the magnitude of the total photon counts, thus making it more difficult to generate a histogram of high quality. Unless there is a certain number of total counts, RM yields a poor estimate of the mean lifetime (15,16). In these cases (15–17), probability-based methods, such as maximum likelihood (ML), provide considerable improvement over RM. One of the limitations of ML, however, is that it assumes a uniform probability distribution of the parameters describing the fluorescence decay function. Thus, ML can be further improved by implementing a suitable *nonuniform* distribution. In this context, we note that alternative approaches such as phasor-based methods (18–21) have been adopted in fluorescence-lifetime imaging microscopy, especially, for biological samples. These methods performed well compared to RM methods in terms of computational efficiency and extracting contributions of different components.

Here, we consider photon-counting data analysis using a Bayesian framework, where the distribution of parameters is obtained from both their prior knowledge and the evidence-based likelihood of an event for a given set of parameters. If  $\beta$  and  $E$  represent the parameter space and the evidence (*i.e.* experimental observations), respectively, then the *posterior* distribution of the parameters for  $E$ ,  $P(\beta|E)$ , is given by the Bayes' theorem (22–24):

$$P(\beta|E) = \frac{P(\beta)P(E|\beta)}{P(E)} \quad (1)$$

$P(E|\beta)$  is the likelihood of evidence given the set of parameters  $\beta$ ; and  $P(\beta)$  is the *prior* distribution of the parameters, which is obtained from the prior knowledge of the parameters. As the evidence is collected, the prior knowledge can be updated for the prediction of the parameters.  $P(E)$  is the total likelihood (also known as the marginal likelihood) of the evidence at all possible points in the parameter space and acts as a normalization.

The Bayesian method is employed (23,25–38) to estimate parameters where there are insufficient evidences. It has been used in fluorescence-lifetime imaging (30,32,37), Förster resonance energy transfer (30) and fluorescence correlation spectroscopy (35,36) experiments. The choices, however, of the parameters to which priors are assigned and the functional form of the priors themselves varied widely. In some cases, an

\*Corresponding author e-mail: jwp@iastate.edu (Jacob W. Petrich)  
© 2018 The American Society of Photobiology

exponential prior has been assigned to “the relaxation time of the photon-generating emission process” based on the argument that it has the maximum entropy within the allowed parameter range (37). In other cases, a uniform prior was assigned for the fraction of mean lifetime components; but this defeats the point of implementing the Bayesian approach because it becomes reduced to the ML method (30). Thus, one of the major challenges in implementing a Bayesian analysis of photon-counting data is determining the choice of the prior distribution and updating it as more evidence is successively acquired. In this work, we compare *Gaussian* and *exponential* prior distributions, where the lifetime parameter is directly incorporated in the posterior that is to be optimized, as well as *Dirichlet* prior distribution, where the lifetime parameter is indirectly calculated using the estimated probability of the bins. For the Gaussian and exponential prior, two analysis schemes were employed. In one, an identical prior was used for every data trace collected for a fixed number of counts. In the other, the prior is calculated and updated using the statistics of the results obtained from a data trace having a similar number of counts. As the latter method is preferable, the discussion of the former is given in the Supporting Information.

These prior distributions and the utility of the Bayesian approach were tested by analyzing photon-counting data obtained from the very well-characterized fluorophore, rose bengal. Rose bengal in methanol has an excited-state lifetime of  $0.49 \pm 0.01$  ns at room temperature (15). Three sets of data were collected, each consisting of 50 individual traces, with a total number of counts of approximately 20, 200 and 20 000, respectively. In all the analyses, we incorporated the real instrument response function (IRF), a very narrow ~20-ps time channel (to avoid the limitations incurred from binning time channels (15)) and a shift parameter.

## MATERIALS AND METHODS

Rose bengal (Sigma-Aldrich, St. Louis) was purified by thin-layer chromatography (15). 550 nm was the excitation wavelength. Time-resolved data were collected using a homemade instrument (15). The full width at half-maximum of the instrument function was typically ~120 ps. The data were collected in 1024 channels (bins), providing a time resolution of 19.51 ps/channel and a full-scale time window of 19.98 ns. Three different data sets consisting of 50 fluorescence decay traces were collected with a total number of counts of approximately 20, 200 and 20 000, respectively.

For a single emissive species, the signal from the excited state of the fluorophore is represented by a single-exponential decay. If  $t_j$  is the time after the excitation corresponding to the  $j^{\text{th}}$  time channel, then the fluorescence signal corresponding to that time is given by  $F(t_j) \propto e^{-(t_j/\tau)}$ , where  $\tau$  is the mean excited-state lifetime (*i.e.* the lifetime) of the fluorophore. Let  $\mathbf{C} = (c_1, c_2, \dots, c_K)$  be the set of counts obtained in the  $K = 1024$  bins represented by the time axis,  $\mathbf{t} = (t_1, t_2, \dots, t_K)$ , where the center of the  $j^{\text{th}}$  bin is given by  $t_j$  and the corresponding counts are given by  $c_j$ . Similarly, we experimentally measure the instrument response function (IRF) and represent it as  $\mathbf{I} = (I_1, I_2, \dots, I_K)$ , where the  $I_j$  is the number of counts of the IRF in the  $j^{\text{th}}$  bin. The width of each bin is given by  $\epsilon = 19.51$  ps. In a discretized data collection system, as in time-correlated, single-photon counting, the probability that a photon is detected in the  $j^{\text{th}}$  bin,  $p_j$ , is proportional to the discrete convolution of the IRF and the model for the fluorescence decay function,  $F(t_j)$ .

$$p_j(\tau, b) \propto \sum_{i=1}^{j-j_0-1} I_i F(t_j - t_i - b) = \sum_{i=1}^{j-j_0-1} I_i e^{-\left(\frac{t_j - t_i - b}{\tau}\right)} \quad (2)$$

where  $b$  is a parameter that assumes continuous values,  $j_0$  is an integer and the relation between them is given by  $b = j_0\epsilon + \zeta$ , where  $\zeta$  lies between 0 and  $\epsilon$ , the time width of the bin.  $b$  describes the linear shift between the instrument response function and the fluorescence decay (15). If  $\hat{\mathbf{C}} = (\hat{c}_1, \hat{c}_2, \dots, \hat{c}_K)$  represents the predicted counts from the

convoluted exponential model, then the number of predicted counts in the  $j^{\text{th}}$  bin,  $\hat{c}_j$ , is given by:

$$\hat{c}_j = C_T p_j(\tau, b) = C_T \frac{\sum_{i=1}^{j-j_0-1} I_i e^{-\left(\frac{t_j - t_i - b}{\tau}\right)}}{\sum_{k=1}^K \left( \sum_{i=1}^{k-j_0-1} I_i e^{-\left(\frac{t_k - t_i - b}{\tau}\right)} \right)} \quad (3)$$

where  $C_T = \sum_j c_j$ , the total number of counts.

At this point, we note that many time-resolved technique based on single-photon counting, as for example STED with a continuous-wave depletion laser, implements “time-gating” (39,40). This gating eliminates the early part of the decay. This might be advantageous for the analysis by the traditional RM-based fitting methods since it avoids the problem of deconvolution of the time-resolved data and other instrumental issues, for example, those related to depletion. Loosing the early part of the decay, however, may influence the estimation of the lifetimes, especially if there are any shorter lifetime components. By incorporating the experimental IRF in our analysis, we eliminated the instrumental artifact without losing the dynamic range. Time-gating also decreases the number of total photons counts. We are exploring the effect of the number of total photon counts in this study without sacrificing the early part of the decay.

## The likelihood of the collected data and the Bayesian formulation

The likelihood of observing a sequence of counts  $(c_1, c_2, \dots, c_K)$  with probability  $(p_1, p_2, \dots, p_K)$  for a given set of parameters  $(\tau, b)$  and subject to the condition,  $C_T = \sum_j c_j$ , is given by the multinomial form (15–17):

$$P(c_1, c_2, \dots, c_K | \tau, b) = \frac{C_T!}{c_1! c_2! \dots c_K!} \prod_{j=1}^K (p_j)^{c_j} = C_T! \prod_{j=1}^K \frac{(p_j)^{c_j}}{c_j!} \quad (4)$$

Using Eq. (3) for the probability,  $p_j = \hat{c}_j / C_T$ , we obtain:

$$P(c_1, c_2, \dots, c_K | \tau, b) = C_T! \prod_{j=1}^K \frac{(\hat{c}_j / C_T)^{c_j}}{c_j!} \quad (5)$$

Note that both the probability of a photon being detected in the  $j^{\text{th}}$  channel,  $p_j$ , and the predicted counts,  $\hat{c}_j$ , in that channel are functions of the parameters  $\tau$  and  $b$ . The experimental data, the “evidence” of photon-counting events for a given parameter space  $\boldsymbol{\beta} \equiv (\tau, b)$ , are the observed counts. Therefore, we have  $\mathbf{E} \equiv \mathbf{C} = (c_1, c_2, \dots, c_K)$ ; and Eq. (5) can be rewritten as:

$$P(\mathbf{E} | \boldsymbol{\beta}) = C_T! \prod_{j=1}^K \frac{(\hat{c}_j / C_T)^{c_j}}{c_j!} \quad (6)$$

*Gaussian and exponential prior distributions.* The critical part of the Bayesian analysis is identifying and selecting a suitable prior distribution for the parameters. Since our analysis includes two independent parameters,  $\tau$  and  $b$ , the prior distribution is:

$$P(\boldsymbol{\beta}) = P(\tau)P(b). \quad (7)$$

We have shown that the estimated mean lifetime of a fluorophore approximately follows a normal distribution (15,16). This conclusion is also obtained from the central limit theorem (41,42), which states that with a sufficiently large number of samples or of observations the distribution will converge to a normal distribution. Therefore, a Gaussian function with a preselected mean and variance is arguably a good choice for a prior distribution:

$$P(\tau) = (2\pi\sigma_0^2)^{-1/2} e^{-\left[\frac{(\tau - \mu_0)^2}{2\sigma_0^2}\right]}. \quad (8)$$

The “hyperparameters” (*i.e.* the parameters determining the distribution of the parameter  $\tau$ )  $\mu_0$  and  $\sigma_0$  are the mean and the standard deviation of the prior distribution for  $\tau$ . We also have tested the exponential prior distribution for the mean lifetime with known hyperparameter,  $\lambda_0$ :

$$P(\tau) = \lambda_0 e^{-\lambda_0 \tau}, \quad (9)$$

where  $\langle \tau \rangle = 1/\lambda_0$  is the mean of the prior distribution. For the shift parameters,  $b$ , since we limit ourselves to a small range,  $-0.1$  to  $0.1$  ns, it is convenient to assume that their distribution is uniform. Therefore, we take  $P(b) = 1/(b_{\max} - b_{\min})$ , which is a constant and does not affect the overall prior distribution,  $P(\beta)$ . From Eq. (1), we write:

$$P(\beta|E) = \frac{P(\tau)P(b)P(E|\beta)}{P(E)} \quad (10)$$

The marginal likelihood,  $P(E)$ , is given its name from the process of “marginalization,” which is an integration over all the parameters (27):

$$P(\beta|E) = \frac{P(\tau)P(b)P(E|\beta)}{\int d\tau db P(\tau)P(b)P(E|\tau, b)} \quad (11)$$

Since  $P(b)$  is a constant, it can be eliminated from Eq. (11). Substituting  $P(\tau)$  from Eq. (8) and the expression for  $P(E|\beta)$  from Eq. (6), the logarithm of the posterior for the Gaussian prior distribution can be written as:

$$\ln P(\beta|E) = \gamma_1 - \frac{(\tau - \mu_0)^2}{2\sigma_0^2} + \sum_{j=1}^K c_j \ln \hat{c}_j \quad (12)$$

where all the terms that are independent of the parameters  $\tau$  and  $b$  are condensed into the constant  $\gamma_1$ . Similarly, if we choose the exponential prior distribution for the mean lifetime given in Eq. (9), we have:

$$\ln P(\beta|E) = \gamma_2 - \lambda_0 \tau + \sum_{j=1}^K c_j \ln \hat{c}_j, \quad (13)$$

where  $\gamma_2$  is another constant, independent of the parameters  $\tau$  and  $b$ . Maximization, therefore, of the logarithm of the posterior probability distribution in Eqs. (12) and (13) provides the optimum values of the parameters.

**Dirichlet prior distribution.** Since the joint probability distribution given in Eq. (4) is in multinomial form, the Dirichlet prior (43–49) distribution is a natural choice for estimating the probability of the channels because it forms a conjugate prior (48,49) with the multinomial distribution insofar as it combines with the likelihood function to form a posterior distribution that belongs to same Dirichlet family. Thus, analytical solutions for the parameters can be easily formulated. The process for extracting the lifetime from the estimated probabilities of the channels is the following. We rewrite the likelihood distribution function from Eq. (4) as  $P(c|\pi)$  in the following by considering the probabilities of the channels as unknown parameters given by  $\pi = (\pi_1, \pi_2, \dots, \pi_K)$ , where  $\sum_j \pi_j = 1$ .

$$P(c|\pi) = C_T! \prod_{j=1}^K \frac{(\pi_j)^{c_j}}{c_j!}. \quad (14)$$

Let  $\alpha = (\alpha_1, \alpha_2, \dots, \alpha_K)$  be the “precounts” (virtual counts (48) or pseudo counts (49)) of the channels with probabilities  $(\pi_1, \pi_2, \dots, \pi_K)$  before the evidence is collected; and let the sum of all “precounts” be  $\sum_j \alpha_j = A_T$ . Then, the Dirichlet prior distribution is:

$$P(\pi|\alpha) \sim D(\alpha_1, \alpha_2, \dots, \alpha_K) = \frac{\Gamma(A_T)}{\prod_{j=1}^K \Gamma(\alpha_j)} \prod_{j=1}^K \pi_j^{\alpha_j-1} \quad (15)$$

The “precounts,”  $\alpha$ , function as hyperparameters for the  $\pi$ . The Dirichlet prior mean and variance are given by  $E(\pi_j) = \alpha_j/A_T$  and  $\text{Var}(\pi_j) = \alpha_j(A_T - \alpha_j)/A_T^2(A_T + 1)$ , respectively (43).

The posterior is given by

$$P(\pi|c, \alpha) \propto P(\pi|\alpha)P(c|\pi) \sim D(\alpha_1 + c_1, \alpha_2 + c_2, \dots, \alpha_K + c_K) \\ = \frac{\Gamma(A_T + C_T)}{\prod_{j=1}^K \Gamma(\alpha_j + c_j)} \prod_{j=1}^K \pi_j^{\alpha_j + c_j - 1} \quad (16)$$

and the posterior mean is given by

$$E(\pi_j|c) = \frac{\alpha_j + c_j}{A_T + C_T} = \frac{A_T}{A_T + C_T} \theta_j + \frac{C_T}{A_T + C_T} \phi_j \quad (17)$$

where,  $\theta_j = E(\pi_j) = \alpha_j/A_T$  and  $\phi_j = c_j/C_T$ . The posterior mean is thus the weighted average of the prior mean  $\theta_j$  and the sample mean  $\phi_j$  with respect to the total “precounts” and the total experimental counts, respectively (43,45). The most important aspect of the Dirichlet prior is that, unlike the Gaussian and exponential priors, it does not combine the prior distribution of the lifetime parameter ( $\tau$ ) directly in the estimation. Rather, the method of employing a Dirichlet prior evaluates the expected probability of the channels given the experimental counts.

In order to find the lifetime parameter, the bin-averaged time of the photon counts data was evaluated from the posterior and then compared with the same quantity calculated from the convoluted model. In order to do this, first, one needs to estimate the “precounts” of the channels. For a given set of initial parameters ( $\tau_{\text{int}}, b_{\text{int}}$ ), we propose to distribute the total number of experimental counts  $C_T$  into the  $K$  bins to estimate  $\alpha = (\alpha_1, \alpha_2, \dots, \alpha_K)$  as follows, using Eq. (3):

$$\alpha_j = C_T p_j(\tau_{\text{int}}, b_{\text{int}}) = C_T \frac{\sum_{i=1}^{j-j_0-1} I_i e^{-\left(\frac{j-j_0-b_{\text{int}}}{\tau_{\text{int}}}\right)}}{\sum_{k=1}^K \left( \sum_{i=1}^{k-j_0-1} I_i e^{-\left(\frac{k-j_0-b_{\text{int}}}{\tau_{\text{int}}}\right)} \right)} \quad (18)$$

where  $\sum_j \alpha_j = A_T = C_T$ . The expectation values of the bin probabilities  $\pi_j$  are then calculated using Eq. (17) for all the channels. Let  $t_{\text{av}}$  represent the bin-averaged time calculated from the expectation value of the bin probability. Therefore,

$$t_{\text{av}} = \sum_{j=1}^K t_j E(\pi_j|c) = \sum_{j=1}^K t_j \frac{\alpha_j + c_j}{A_T + C_T} \quad (19)$$

Similarly, for a given set of values of the parameters ( $\tau, b$ ), we can define another bin-averaged time ( $t'_{\text{av}}$ ) for the convoluted model using the form of the probability  $p_j$  given in Eq. (3):

$$t'_{\text{av}} = \sum_{j=1}^K t_j p_j(\tau, b) = \sum_{j=1}^K t_j \frac{\sum_{i=1}^{j-j_0-1} I_i e^{-\left(\frac{j-j_0-b}{\tau}\right)}}{\sum_{k=1}^K \left( \sum_{i=1}^{k-j_0-1} I_i e^{-\left(\frac{k-j_0-b}{\tau}\right)} \right)} \quad (20)$$

Theoretically, the values of these two bin-averaged times ( $t_{\text{av}}$  and  $t'_{\text{av}}$ ) should be equal for the ideal data without any noise. Therefore, for experimental data we can minimize the absolute difference ( $\Delta_{\text{abs}}$ ) between  $t_{\text{av}}$  and  $t'_{\text{av}}$  as shown in Eq. (21) to obtain the optimum values of the parameters ( $\tau_{\text{opt}}, b_{\text{opt}}$ ).

$$\Delta_{\text{abs}} = |t_{\text{av}} - t'_{\text{av}}| \quad (21)$$

The obtained optimal values are set as the new initial parameters,  $(\tau_{\text{int}}, b_{\text{int}}) = (\tau_{\text{opt}}, b_{\text{opt}})$  and the entire procedure is repeated for several iterations until the results converge to a preset tolerance.

## Computational methods

The optimizations of the posterior distributions given in Eqs. (12) and (13) are performed using codes written in MATLAB. (These codes are provided in the SI.) The GlobalSearch toolbox in MATLAB uses the “fmincon” solver to minimize the objective function with respect to the parameters; and in each calculation, a global minimum is reached. The ranges of the parameters  $\tau$  and  $b$  are assigned as 0.01 to 1.5 ns and  $-0.1$

to 0.1 ns, respectively. Within the specified ranges, we run our in-house routine with different initial values of the parameters and always retrieve the same results through the third decimal place.

**Gaussian and exponential priors.** Both Eqs. (12) and (13) depend on the initial values of the hyperparameters. We employ two schemes to assign the values of the hyperparameters. In the first, we use identical prior hyperparameters (*i.e.* fixed  $\mu_0$  and  $\sigma_0$  for the Gaussian prior or fixed  $\lambda_0$  for the exponential prior) for all the fifty decay traces in a set. In the second, we update the prior hyperparameters for the analysis of  $N^{\text{th}}$  decay trace using the calculated statistics of the results obtained from all the analyzed  $N - 1$  decay traces of that set according to the Eq. (22) given below. In the second scheme, we update the mean and the standard deviation after the analysis of 1 and 5 decay traces, respectively, to obtain sufficient statistics:

$$\begin{aligned} (\mu_0)_N &= \frac{1}{N-1} \sum_{r=1}^{N-1} \tau_r; \quad \text{for all } N > 1 \\ (\sigma_0)_N &= \sqrt{\frac{1}{N-2} \sum_{r=1}^{N-1} [\tau_r - (\mu_0)_N]^2}; \quad \text{for all } N > 2 \\ (\lambda_0)_N &= 1/(\mu_0)_N; \quad \text{for all } N > 1 \end{aligned} \quad (22)$$

In both schemes, different combinations of the initial values of the hyperparameters are assigned.

**Dirichlet prior.** As shown in Eq. (21), the absolute difference between  $t_{\text{av}}$  and  $t'_{\text{av}}$  is minimized to obtain the new set of initial parameters  $(\tau_{\text{int}}, b_{\text{int}}) = (\tau_{\text{opt}}, b_{\text{opt}})$ . The change of the value of the lifetime parameter is monitored; and convergence is obtained if the change between two successive iterations,  $\delta\tau$ , is less than a preset tolerance value, which we set to  $\delta\tau_{\text{tol}} = 10^{-4}$  ns. If  $b < 10^{-4}$  in an iteration, then  $b$  is set to zero. (We find  $b \approx 0$  using the maximum likelihood estimation and other Bayesian analyses considered here for our data sets. Setting  $b = 0$  simplifies the computation.) All the calculations converged in  $\leq 50$  iterations. To test the influence of the initial conditions, the parameter space for the lifetime has been expanded (0.001 to 15 ns), and various initial values of  $\tau_{\text{int}}$  are chosen within that range. In all cases, the results converge to the same lifetime value.

## RESULTS AND DISCUSSION

### Gaussian and exponential priors

We assign the initial values of the hyperparameters for a decay trace and those values are mentioned in the corresponding figures and tables. After obtaining the results from a certain number of traces, we calculate the statistics of the results for all the decay traces considered up to that point using Eq. (22). The calculated statistics provide the hyperparameters for the subsequent analysis of the remaining decay traces. After each step, a new set of hyperparameters is obtained. Estimated lifetimes using this scheme are presented in Fig. 1 for all 50 decay traces for each set of data having a total number of 20, 200 and 20 000 counts, respectively. Each panel is labeled with the initial values of  $\mu_0$  and  $\sigma_0$ . The histograms of the lifetimes obtained by using Gaussian and exponential priors with different sets of initial hyperparameters are given in Fig. 2. Statistics are summarized in Table 1.

For a Gaussian prior, where  $\sigma_0 = 0.5$  ns, the results converge to the correct mean value as more and more decay traces are analyzed for a data set. As a result, the distribution of the estimated lifetimes becomes very narrow, with standard deviations of 8%, 2% and less than 1% of the mean lifetime for the data sets with total number of 20, 200 and 20 000 counts, respectively, as shown in Fig. 2a and Table 1. The identical-prior counterpart (see Supporting Information) has much wider distributions, as noted in the previous section. As in the identical-prior counterpart, however, the estimated lifetime is not very sensitive to the initial values of the prior mean,

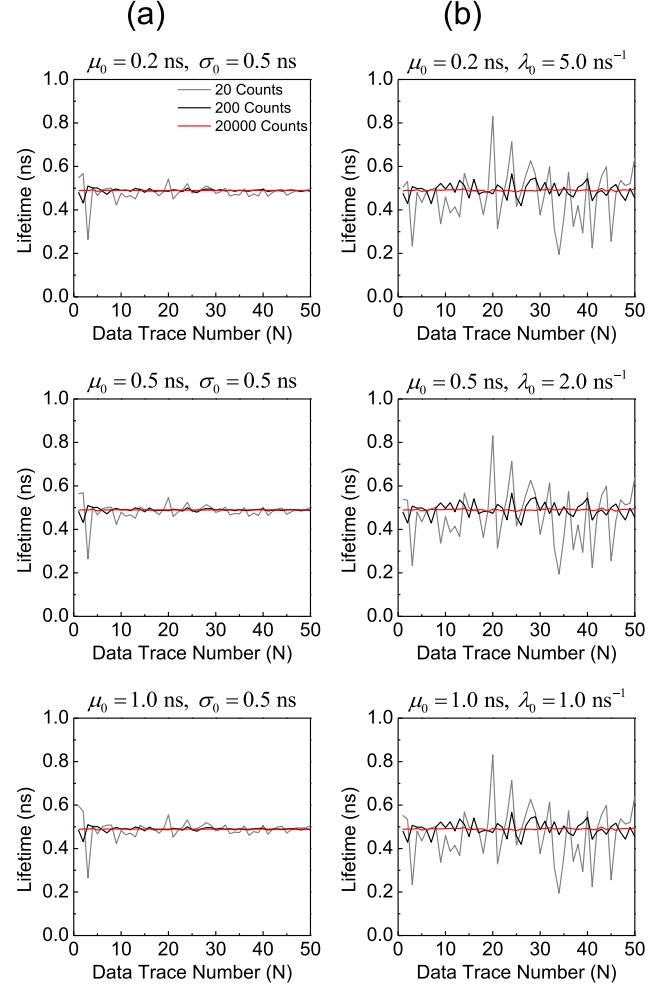


**Figure 1.** Estimated lifetimes of all fifty decay traces obtained by the Bayesian analysis where priors are updated following Eq. (22). The results using a Gaussian prior are shown in column (a); and the results from an exponential prior, in column (b). Corresponding hyperparameters are given at the top of each panel.

$\mu_0$ , when the initial value of the prior standard deviation  $\sigma_0$  is wide. For an exponential prior, the convergence is not as rapid as in the case of the Gaussian prior using this strategy (Fig. 2b). Again, the initial choice of  $\lambda_0$  has no influence on the estimated lifetime for the three data sets. These results also suggest that the Gaussian prior is preferable to the exponential prior.

This example of updating the prior distribution using the results from data sets with the same number of total counts is purely illustrative. The point is that the fitting results can be improved by employing data collected using similar experimental conditions and choosing the prior hyperparameter accordingly. Once obtained, higher-quality data (*e.g.* from a decay trace having 20 000 total counts) can be used to extract the hyperparameters for the prior when analyzing lesser-quality data (*e.g.* from a decay trace having 20 total photon counts). Further updating of the prior might even be unnecessary, since it is possible that one data set of sufficiently high quality can provide a suitable prior. Such higher-quality data sets may be obtained from bulk solutions or from imaging data from STED experiments, for example, using pixels of higher intensity where the experimental conditions and fluorophore environment are similar.



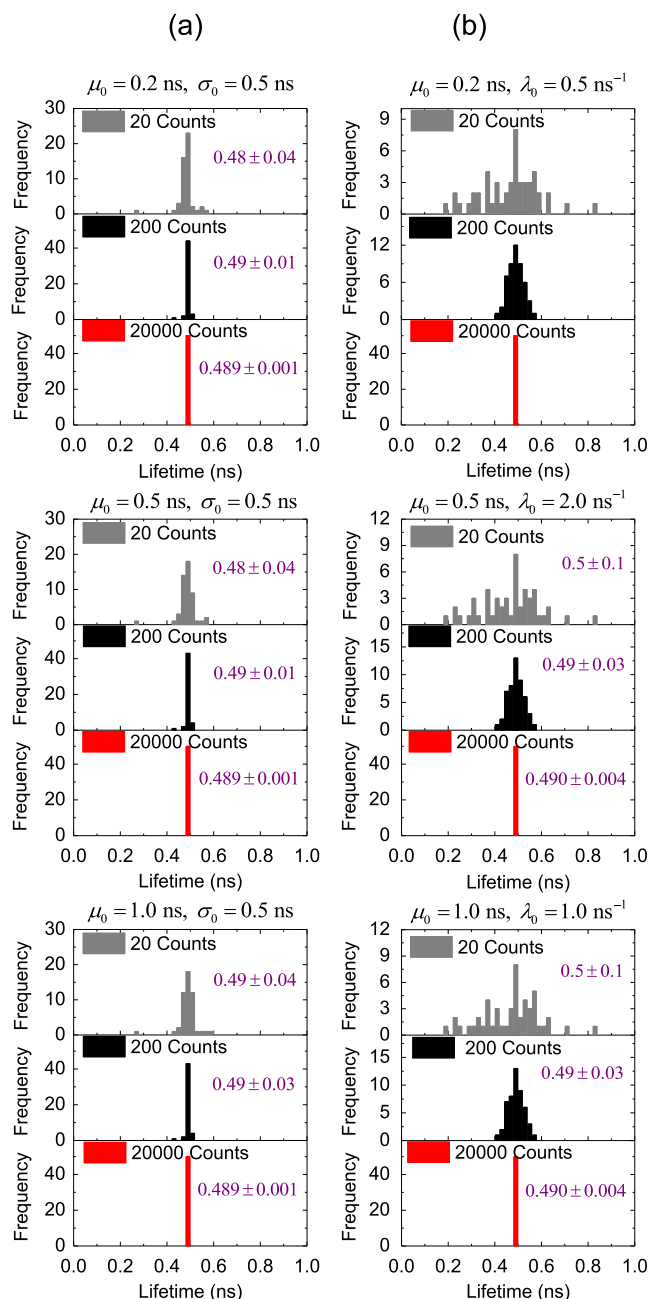


**Figure 2.** Histograms of the estimated lifetimes of all fifty decay traces obtained by the Bayesian analysis using updated priors following Eq. (22). Column (a) represents the results using a Gaussian prior; and column (b), the results using an exponential prior. Corresponding hyperparameters are given at the top of each panel. The mean and the standard deviation of the estimated lifetime are given in each histogram.

### Dirichlet prior

Using the strategy of minimization of the absolute difference between two bin-average time ( $t_{av}$  and  $t'_{av}$ ) given in Eq. (21) for the Dirichlet prior, each of the decay traces was analyzed; and convergence was obtained when  $\delta\tau < 10^{-4}$  ns. The lifetimes of the individual traces are given in Figure S3 for all the decay

traces. The histograms of the lifetimes obtained from an analysis employing the Dirichlet prior are given in Fig. 3 for all the data traces for a given initial condition. The statistics of the results for the fifty decay traces of each set are summarized in Table 2. The value of the initial lifetime ( $\tau_{int}$ ), which has been used to estimate the “precounts” ( $\alpha$ ) for the Dirichlet prior at the beginning of the iteration, is 0.4 ns; and it is given in Fig. 3, Figure S3 and Table 2.

To test the influence of the initial value, the parameter space for the lifetime was expanded ( $0.001$  ns  $\leq \tau_{int} \leq 15$  ns), and various initial values of  $\tau_{int}$  are chosen within that range. In all cases, the results converge to the same lifetime value. An example is shown in Figure S4, where the convergence is tested with various initial conditions ( $\tau_{int}$ ) for a representative data trace randomly chosen from each of the data set with total number of counts 20, 200 and 20 000, respectively.

It can be seen (Tables 2 and S1) that the mean and the standard deviation of the lifetimes obtained for all the fifty decay traces in a set using a Dirichlet prior are comparable to those obtained using a Gaussian prior when  $\sigma_0$  is 0.5 ns in the case of the three values (0.2 ns, 0.5 ns and 1.0 ns) of  $\mu_0$ . When  $\sigma_0$  is 0.3 ns, the statistical results of the lifetimes are comparable to those we obtained from the Dirichlet prior for all cases except that where  $\mu_0$  is 1.0 ns and the data set has 20 total counts. Here, the Gaussian prior yields  $0.6 \pm 0.1$  ns and the Dirichlet prior yields  $0.5 \pm 0.1$  ns. As mentioned above, the statistical results of the lifetimes for the Gaussian prior analysis depend on the value of  $\mu_0$  when  $\sigma_0$  is 0.1 ns for the data set with a total number of counts of 200 or less. On the other hand, the statistical results of the lifetimes obtained from the Dirichlet prior analysis are comparable to those we obtained using an exponential prior for all cases except that where the exponential prior parameter ( $\lambda_0$ ) is  $5.0$  ns $^{-1}$  and the data set has 20 total counts. Here, the exponential prior yields  $0.4 \pm 0.1$  ns.

Thus, the advantage of employing a Dirichlet prior is not so much for the result it yields but rather because its use does not require any *a priori* knowledge of the lifetime of the sample. The change of the value of the lifetime parameter between two successive iterations,  $\delta\tau$ , should converge to yield the optimized results from any given starting point (initial value) for all the three data sets we have considered with total number of counts 20, 200 and 20 000, respectively. The Gaussian prior, on the other hand, can yield much smaller standard deviations, but its use requires prior knowledge of the parameters. In the case of the exponential prior, the initial condition (the value of the hyperparameter,  $\lambda_0$ ) has little influence on the estimated lifetimes for the data set with a total count number of 20. The Dirichlet prior, being a natural conjugate prior for the multinomial distribution, combines with the joint probability of the data obtained in the photon-counting experiments to estimate the posterior of channel probability parameters analytically. It also differs significantly from the Gaussian and exponential prior cases in how the parameters are evaluated.

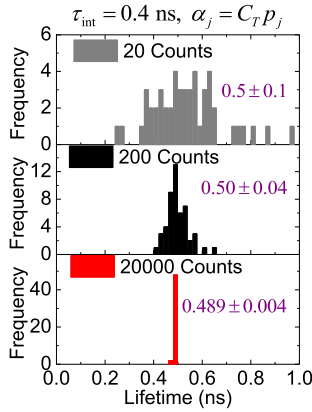
### CONCLUSIONS

We have formulated and demonstrated the usefulness of a Bayesian approach for analyzing time-correlated, single-photon-counting data to estimate the mean fluorescence lifetime of a well-characterized fluorophore, rose bengal. Although the exponential

**Table 1.** Fitting results for three sets of 50 decay traces employing a Bayesian analysis using updated prior distributions.

Total number of counts	Mean lifetime $\pm$ one standard deviation (ns)*		
<b>Gaussian prior</b>	$\mu_0 = 0.2$ ns, $\sigma_0 = 0.5$ ns	$\mu_0 = 0.5$ ns, $\sigma_0 = 0.5$ ns	$\mu_0 = 1.0$ ns, $\sigma_0 = 0.5$ ns
20	$0.48 \pm 0.04$	$0.48 \pm 0.04$	$0.49 \pm 0.04$
200	$0.49 \pm 0.01$	$0.49 \pm 0.01$	$0.49 \pm 0.01$
20 000	$0.489 \pm 0.001$	$0.489 \pm 0.001$	$0.489 \pm 0.001$
<b>Exponential prior</b>	$\lambda_0 = 5.0$ ns <sup>-1</sup>	$\lambda_0 = 2.0$ ns <sup>-1</sup>	$\lambda_0 = 1.0$ ns <sup>-1</sup>
20	$0.5 \pm 0.1$	$0.5 \pm 0.1$	$0.5 \pm 0.1$
200	$0.49 \pm 0.03$	$0.49 \pm 0.03$	$0.49 \pm 0.03$
20 000	$0.490 \pm 0.004$	$0.490 \pm 0.004$	$0.490 \pm 0.004$

\*Mean lifetime  $\pm$  one standard deviation (ns) of fifty decay traces calculated using a Bayesian analysis for three data sets with a total number of counts of 20, 200 and 20 000, respectively. The priors for a data trace in a set are updated using the statistics of the results of all the analyzed decay traces of that set, as given in Eq. (22). The type of prior and the initial values of the hyperparameters are given in the shaded rows.

**Figure 3.** Histograms of the estimated lifetimes of all fifty decay traces obtained by the Bayesian analysis using a Dirichlet prior distribution. The initial values of the lifetime,  $\tau_{\text{int}}$ , and the estimation of the “pre-counts” are given at the top of the panel. The mean and the standard deviation of the estimated lifetimes are given in each histogram.**Table 2.** Fitting results for three sets of 50 decay traces employing a Bayesian analysis using Dirichlet prior distributions.

Total number of counts	Mean lifetime $\pm$ one standard deviation (ns)*
<b>Dirichlet prior</b>	$\tau_{\text{int}} = 0.4$ ns, $\alpha_j = C_T p_j$
20	$0.5 \pm 0.1$
200	$0.50 \pm 0.04$
20 000	$0.489 \pm 0.004$

\*Mean lifetime  $\pm$  one standard deviation (ns) of fifty decay traces calculated using a Bayesian analysis for three data sets with a total number of counts of 20, 200 and 20 000, respectively. The absolute difference between  $t_{\text{av}}$  and  $t'_{\text{av}}$  shown in Eq. (21) is minimized to obtain optimum values of the lifetime, and the convergence is obtained if the change between two successive iteration,  $\delta\tau < 10^{-4}$  ns. The initial parameter,  $\tau_{\text{int}}$ , and the estimation of “precounts” are given in the shaded row.

prior is less sensitive to the initial values of the hyperparameters, the Gaussian prior yields a much narrower distribution of the estimated lifetime and, thus, a more precise value of the retrieved value of the fluorescence lifetime. The greatest advantage, however, of the Dirichlet prior is that for the cases we investigated, the same optimized results are obtained *regardless of the initial conditions* for the prior parameters. Thus, an analysis strategy is suggested in which parameter space can rapidly be searched with the Dirichlet prior, and a subsequent, more refined search may be carried out with a Gaussian or exponential prior, if necessary.

**Acknowledgements**—Support was provided by the U.S. Department of Energy, Office of Science, Office of Biological and Environmental Research, through the Ames Laboratory, under Contract No. DE-AC02-07CH11358. The Ames Laboratory is operated for the U.S. Department of Energy by Iowa State University. We thank Dr. Hyung Jun Woo for encouraging the consideration of the Dirichlet prior and for his helpful comments.

## SUPPORTING INFORMATION

Additional supporting information may be found online in the Supporting Information section at the end of the article:

**Figure S1.** Estimated lifetimes of all decay traces obtained by the Bayesian analysis where identical priors are used.

**Figure S2.** Histograms of the estimated lifetimes of all the decay traces obtained by the Bayesian analysis where identical priors are used.

**Figure S3.** Estimated lifetimes of all fifty decay traces obtained by the Bayesian analysis using a Dirichlet prior distribution.

**Figure S4.** A representative trace from each data set is analyzed using a Dirichlet prior with various initial values ( $\tau_{\text{int}}$ ).

**Table S1.** Fitting results for three sets of 50 decay traces employing a Bayesian analysis using identical prior distributions.

## REFERENCES

- O'Connor, D. V. and D. Phillips (1984) *Time Correlated Single Photon Counting*. Academic Press Inc., London.
- Bastiaens, P. I. and A. Squire (1999) Fluorescence lifetime imaging microscopy: Spatial resolution of biochemical processes in the cell. *Trends Cell Biol.* **9**, 48–52.
- Elangovan, M., R. Day and A. Periasamy (2002) Nanosecond fluorescence resonance energy transfer-fluorescence lifetime imaging microscopy to localize the protein interactions in a single living cell. *J. Microsc.* **205**, 3–14.
- Tinnefeld, P., V. Buschmann, D. P. Herten, K. T. Han and M. Sauer (2000) Confocal fluorescence lifetime imaging microscopy (FLIM) at the single molecule level. *Single Mol.* **1**, 215–223.
- Gerritsen, H., M. Asselbergs, A. Agronskaia and W. Van Sark (2002) Fluorescence lifetime imaging in scanning microscopes: Acquisition speed, photon economy and lifetime resolution. *J. Microsc.* **206**, 218–224.
- Lee, M., J. Tang and R. M. Hochstrasser (2001) Fluorescence lifetime distribution of single molecules undergoing Förster energy transfer. *Chem. Phys. Lett.* **344**, 501–508.
- Scholes, G. D. (2003) Long-range resonance energy transfer in molecular systems. *Annu. Rev. Phys. Chem.* **54**, 57–87.

8. Van Der Meer, B. W., G. Coker and S.-Y. S. Chen (1994) *Resonance Energy Transfer: Theory and Data*. VCH, New York.
9. Thompson, N. L. (2002) *Fluorescence Correlation Spectroscopy*. Springer, Boston, MA.
10. Elson, E. L. and D. Magde (1974) Fluorescence correlation spectroscopy. I. Conceptual basis and theory. *Biopolymers* **13**, 1–27.
11. Magde, D., E. L. Elson and W. W. Webb (1974) Fluorescence correlation spectroscopy. II. An experimental realization. *Biopolymers* **13**, 29–61.
12. Lesoine, M. D., U. Bhattacharjee, Y. Guo, J. Vela, J. W. Petrich and E. A. Smith (2013) Subdiffraction, luminescence-depletion imaging of isolated, giant, CdSe/CdS nanocrystal quantum dots. *J. Phys. Chem. C* **117**, 3662–3667.
13. Lesoine, M. D., S. Bose, J. W. Petrich and E. A. Smith (2012) Supercontinuum stimulated emission depletion fluorescence lifetime imaging. *J. Phys. Chem. B* **116**, 7821–7826.
14. Syed, A., M. D. Lesoine, U. Bhattacharjee, J. W. Petrich and E. A. Smith (2014) The number of accumulated photons and the quality of stimulated emission depletion lifetime images. *Photochem. Photobiol.* **90**, 767–772.
15. Santra, K., J. Zhan, X. Song, E. A. Smith, N. Vaswani and J. W. Petrich (2016) What is the best method to fit time-resolved data? A comparison of the residual minimization and the maximum likelihood techniques as applied to experimental time-correlated, single-photon counting data. *J. Phys. Chem. B* **120**, 2484–2490.
16. Santra, K., E. A. Smith, J. W. Petrich and X. Song (2017) Photon counting data analysis: Application of the maximum likelihood and related methods for the determination of lifetimes in mixtures of rose Bengal and Rhodamine B. *J. Phys. Chem. A* **121**, 122–132.
17. Baker, S. and R. D. Cousins (1984) Clarification of the use of chi-square and likelihood functions in fits to histograms. *Nucl. Instr. Meth. Phys. Res.* **221**, 437–442.
18. Fereidouni, F., A. Esposito, G. Blab and H. Gerritsen (2011) A modified phasor approach for analyzing time-gated fluorescence lifetime images. *J. Microsc.* **244**, 248–258.
19. Schrimpf, W., A. Barth, J. Hendrix and D. C. Lamb (2018) Pam: A framework for integrated analysis of imaging, single-molecule, and ensemble fluorescence data. *Biophys. J.* **114**, 1518–1528.
20. Digman, M. A., V. R. Caiolfa, M. Zamai and E. Gratton (2008) The phasor approach to fluorescence lifetime imaging analysis. *Biophys. J.* **94**, L14–L16.
21. Colyer, R. A., C. Lee and E. Gratton (2008) A novel fluorescence lifetime imaging system that optimizes photon efficiency. *Microsc. Res. Techniq.* **71**, 201–213.
22. Koch, K.-R. (1990) *Bayes' Theorem*. Springer, Berlin, Germany.
23. Bishop, C. M. (2006) *Pattern Recognition and Machine Learning*. Springer, New York, NY.
24. Lindley, D. V. (1991) *Making Decisions*. John Wiley & Sons, London, UK.
25. Bretthorst, G. L. and U. V. Toussaint. The maximum entropy method of moments and Bayesian probability theory. Vol. **1553**, pp. 3–15. AIP, Proceedings of the AIP Conf. Proc. 2013.
26. Wakefield, J. (1996) The bayesian analysis of population pharmacokinetic models. *J. Am. Stat. Assoc.* **91**, 62–75.
27. Bretthorst, G. L. (1990) *An Introduction to Parameter Estimation using Bayesian Probability Theory*. Springer, Dordrecht, Netherlands.
28. Lai, W., X. Liu, W. Chen, X. Lei, X. Tang and Z. Zang (2015) Transient multiexponential signals analysis using Bayesian deconvolution. *Appl. Math. Comp.* **265**, 486–493.
29. Barber, P., S. Ameer-Beg, S. Pathmanathan, M. Rowley and A. Coolen (2010) A Bayesian method for single molecule, fluorescence burst analysis. *Biomed. Opt. Express.* **1**, 1148–1158.
30. Kaye, B., P. J. Foster, T. Y. Yoo and D. J. Needleman (2017) Developing and testing a Bayesian analysis of fluorescence lifetime measurements. *PLoS ONE* **12**, e0169337.
31. Van Dyk, D. A., A. Connors, V. L. Kashyap and A. Siemiginowska (2001) Analysis of energy spectra with low photon counts via Bayesian posterior simulation. *Astrophys. J.* **548**, 224.
32. Rowley, M. I., A. C. Coolen, B. Vojnovic and P. R. Barber (2016) Robust Bayesian fluorescence lifetime estimation, decay model selection and instrument response determination for low-intensity FLIM imaging. *PLoS ONE* **11**, e0158404.
33. Malave, P. and A. Sitek (2015) Bayesian analysis of a one-compartment kinetic model used in medical imaging. *J. Appl. Stat.* **42**, 98–113.
34. Borsuk, M. E. and C. A. Stow (2000) Bayesian parameter estimation in a mixed-order model of BOD decay. *Water Res.* **34**, 1830–1836.
35. Guo, S.-M., J. He, N. Monnier, G. Sun, T. Wohland and M. Bathe (2012) Bayesian approach to the analysis of fluorescence correlation spectroscopy data II: Application to simulated and in vitro data. *Anal. Chem.* **84**, 3880–3888.
36. He, J., S.-M. Guo and M. Bathe (2012) Bayesian approach to the analysis of fluorescence correlation spectroscopy data I: Theory. *Anal. Chem.* **84**, 3871–3879.
37. Rowley, M. I., P. R. Barber, A. C. Coolen and B. Vojnovic. Bayesian analysis of fluorescence lifetime imaging data. Vol. **7903**, pp. 790325–790325. International Society for Optics and Photonics, Proceedings of the SPIE BiOS2011.
38. Lubrano, M. Bayesian analysis of nonlinear time series models with a threshold. Vol. **11**, pp. 79. Cambridge University Press, Proceedings of the Nonlinear Econometric Modeling in Time Series: Proceedings of the Eleventh International Symposium in Economic Theory 2000.
39. Moffitt, J. R., C. Osseforth and J. Michaelis (2011) Time-gating improves the spatial resolution of STED microscopy. *Opt. Express* **19**, 4242–4254.
40. Vicidomini, G., G. Moneron, K. Y. Han, V. Westphal, H. Ta, M. Reuss, J. Engelhardt, C. Eggeling and S. W. Hell (2011) Sharper low-power STED nanoscopy by time gating. *Nat. Methods* **8**, 571.
41. Dobrushin, R. L. (1956) Central limit theorem for nonstationary markov chains. I. *Theory Probab. Appl.* **1**, 65–80.
42. Feller, W. (1968) *An Introduction to Probability Theory and its Applications: Volume I*. John Wiley & Sons, Inc., London-New York-Sydney-Toronto.
43. Agresti, A. (2010) *Analysis of Ordinal Categorical Data*. John Wiley & Sons, Hoboken, NJ.
44. Minka, T. P. (2000) Estimating a Dirichlet distribution. Technical report, MIT.
45. Agresti, A. and D. B. Hitchcock (2005) Bayesian inference for categorical data analysis. *Stat. Meth. Appl.* **14**, 297–330.
46. Basu, D. and D. B. Hitchcock (1982) On the Bayesian analysis of categorical data: The problem of nonresponse. *J. Stat. Plann. Inference* **6**, 345–362.
47. Huang, J. (2005) Maximum likelihood estimation of Dirichlet distribution parameters. *CMU Technique Report*.
48. Minka, T. P. (2003) Bayesian inference, entropy, and the multinomial distribution. *Online tutorial*.
49. Murphy, K. P. (2006) *Binomial and Multinomial Distributions*. University of British Columbia, Tech. Rep.